

The Duration of Non-flow Periods Influences the Dynamic Responses of Biofilm Metabolic Activities to Flow Rewetting

Lingzhan Miao¹, chaoran LI², Tanveer M Adyel³, Zhilin Liu¹, Jun Wu¹, Songqi Liu¹, Wanyi Li¹, and Jun Hou¹

¹Hohai University

²

³Deakin University

November 22, 2022

Abstract

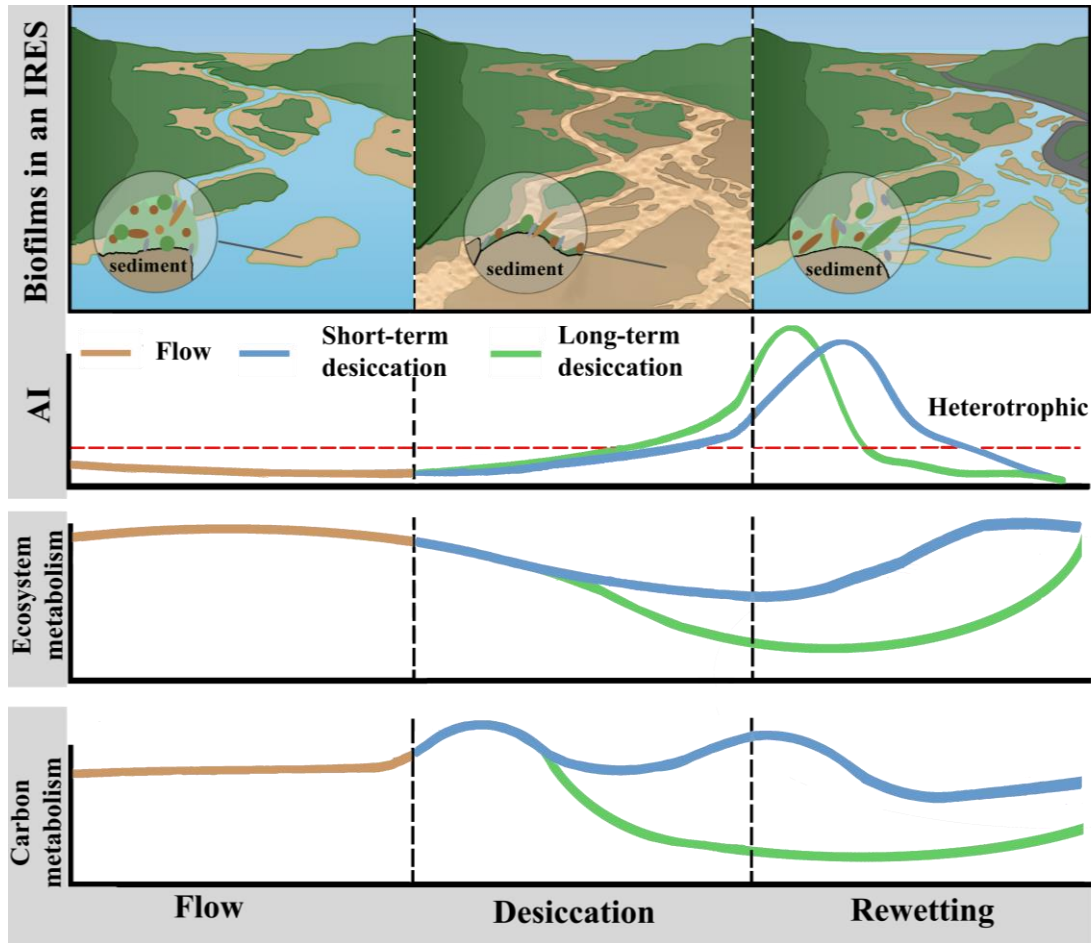
Global change has led to the increased duration and frequency of droughts and may affect the microbial-mediated biochemical processes of intermittent rivers and ephemeral streams (IRES). Effects of flow desiccation on the physical structure and community structure of benthic biofilms of IRES have been addressed, however the dynamic responses of biofilm functions related to ecosystem processes during the dry-wet transition remain poorly understood. Herein, dynamic changes in biofilm metabolic activities were investigated during short-term (25-day) and long-term (90-day) desiccation, both followed by a 20-day rewetting period. Distinct response patterns of biofilm metabolism were observed based on flow conditions. Specifically, biofilms were completely desiccated after 10 days of drying. Biofilm ecosystem metabolism, represented by the ratio of gross primary production (GPP) and community respiration (CR), was significantly inhibited during desiccation and gradually recovered back to autotrophic after rewetting due to the high resilience of GPP. Also, the potential metabolic activities of biofilms were maintained during desiccation and showed a tendency to recover after rewetting. While long-term desiccation caused irreparable damage to the total carbon metabolism of biofilms that could not be recovered to the control level even after 20 days of rewetting. Moreover, the metabolic activities of amine and amino acids showed an inconsistent pattern of recovery with total carbon metabolism, indicating the development of selective carbon metabolism. This research provides direct evidence that the increased non-flow periods affects biofilm-mediated carbon biogeochemical processes, which should be taken into consideration for the decision-making of the ecological and environmental flow of IRES.

Hosted file

supporting-information 0903.docx available at <https://authorea.com/users/536130/articles/598958-the-duration-of-non-flow-periods-influences-the-dynamic-responses-of-biofilm-metabolic-activities-to-flow-rewetting>

26

• Graphical Abstract



27
28

•

29 **Abstract**

30 Global change has led to the increased duration and frequency of droughts and may affect
31 the microbial-mediated biochemical processes of intermittent rivers and ephemeral streams
32 (IRES). Effects of flow desiccation on the physical structure and community structure of benthic
33 biofilms of IRES have been addressed, however the dynamic responses of biofilm functions
34 related to ecosystem processes during the dry-wet transition remain poorly understood. Herein,
35 dynamic changes in biofilm metabolic activities were investigated during short-term (25-day)
36 and long-term (90-day) desiccation, both followed by a 20-day rewetting period. Distinct
37 response patterns of biofilm metabolism were observed based on flow conditions. Specifically,
38 biofilms were completely desiccated after 10 days of drying. Biofilm ecosystem metabolism,
39 represented by the ratio of gross primary production (GPP) and community respiration (CR), was
40 significantly inhibited during desiccation and gradually recovered back to autotrophic after
41 rewetting due to the high resilience of GPP. Also, the potential metabolic activities of biofilms
42 were maintained during desiccation and showed a tendency to recover after rewetting. While
43 long-term desiccation caused irreparable damage to the total carbon metabolism of biofilms that
44 could not be recovered to the control level even after 20 days of rewetting. Moreover, the
45 metabolic activities of amine and amino acids showed an inconsistent pattern of recovery with
46 total carbon metabolism, indicating the development of selective carbon metabolism. This
47 research provides direct evidence that the increased non-flow periods affects biofilm-mediated
48 carbon biogeochemical processes, which should be taken into consideration for the decision-
49 making of the ecological and environmental flow of IRES.

50

51 **Keywords:** Biofilm; intermittent rivers and ephemeral streams; microbial functions; dynamic
52 responses; carbon metabolism

53

54 **1 Introduction**

55 Global climate variabilities and human activities have led to the increasing intermittency
56 of numerous streams and rivers (Acuña et al., 2014, Messenger et al., 2021). Intermittent rivers
57 and ephemeral streams (IRES) are characterized by the alternation of desiccation and rewetting
58 hydrological phases, contributing to the biodiversity and biogeochemical processes (Lv et al.,
59 2017), and functional integrity of fluvial systems (Shumilova et al., 2019, Messenger et al., 2021).
60 However, the increasing flow intermittency has led to a harsh environment for the aquatic
61 organisms, especially the microbial communities, and influences the ecosystem processes
62 ongoing in the IRES (Navarro-Ortega et al., 2015). For instance, benthic biofilms serve as an
63 ecological indicator for coupling the structure and function of the river ecosystem and play a key
64 driving role in the primary production, nutrient circulation, and energy flow of the river system
65 (Sun et al., 2021, Fan et al., 2021). However, unpredictable desiccation may affect the
66 community structure and function of biofilm, which in turn influence the ecosystem processes of
67 the IRES ecosystem (Bogan et al., 2017, Zlatanović et al., 2018).

68 Previous studies have demonstrated that the duration, frequency, and severity of the
69 dehydration could affect the physicochemical properties, community composition, and activities
70 of enzymes in biofilms of aquatic system (Sabater et al., 2016, Shumilova et al., 2019). For
71 example, the alternation of desiccation and rewetting hydrological phases has the greatest
72 influence on the algal community, followed by bacterial, and the least influence on the fungal

73 community in biofilms(Gionchetta et al., 2019). The increasing desiccation periods are reported
74 to extend the ecological niche, and significantly increase the β -diversity of biofilm communities
75 (Feng et al., 2020), while the α -diversity (species richness) decreased significantly in most
76 biofilm communities(Sabater et al., 2016 , Zlatanović et al., 2018). Also, the combination of the
77 temporal components and the severity of the desiccation affected the microbial function of
78 biofilm(Colls et al., 2019), leading to a reduction of extracellular enzymes(Timoner et al., 2012 ,
79 Colls et al., 2019), and promoting biofilm to be more heterotrophy(Acuña et al., 2015).
80 Moreover, several recent studies have shown that the increasing desiccation period and intensity
81 affect the recovery of microbial community structure(Pohlon et al., 2018) and the ecosystem
82 metabolism, the ratio of gross primary production (GPP) and community respiration (CR), of
83 biofilms(Acuña et al., 2015). Due to the importance in ecosystem processes of biofilm functions,
84 recovery of biofilm microbial functions following desiccation should be further considered.

85 However, most previous studies investigated the recovery of the community structure and
86 integrated functions of biofilms after a predetermined experimental cycle, little is known about
87 the dynamic responses of biofilm metabolic activities over time under such conditions. Due to
88 the intrinsic resistance and physiological recovery of biofilm under disturbance (Steven et al.,
89 2021), the question here is whether the microbial function of biofilms can be maintained during
90 the desiccation and then can be recovered to original state after flow rewetting. If so, how long
91 does biofilms take for the function to achieve stability, and this question is related to that
92 whether the setting of the recovery period of biofilms after desiccation in previous studies is
93 reasonable (5-10 days; (Fabian et al., 2018 , Gionchetta et al., 2019 , Shumilova et al., 2019)).
94 More importantly, the ecological indicators, such as GPP, CR, and autotrophic index (AI) used in
95 previous studies can only reflect the integrated functions of biofilms, more detailed indicators
96 (for example, carbon metabolism determined by Biology Eco) should be applied to explore the
97 dynamic responses of biofilm metabolic activities to dry and wet stress in IRES systems.

98 In this study, we aimed to identify the effects of the duration of non-flow periods on the
99 dynamic responses of biofilm microbial functions during the alternation of desiccation and
100 rewetting conditions through indoor simulation experiments. Two desiccation periods (short-
101 term (25-day) and long-term (90-day) of biofilms were performed and both followed by a 20-day
102 rewetting period. During the whole experimental period, indicators of biofilm integrated
103 functions were identified, including AI and ecosystem metabolism (represented by GPP and CR
104 ratio). In addition, Biolog eco was used to provide more detailed information about biofilm
105 carbon metabolisms, such as specific activities of carbon sources and functional diversity. We
106 hypothesized that the response patterns of the integrated indicators (AI and ecosystem
107 metabolism) and carbon metabolism may be different after longer desiccation, changes of
108 different metabolic activities may be consistent in desiccation (i); the recovery rate of biofilm
109 functions in the rewetting period after long-term desiccation should be lower than that after
110 short-term desiccation (ii); and the metabolic activity of biofilm could be restored by rewetting
111 after short-term desiccation, but not after long-term desiccation(iii).

112 **2 Materials and Methods**

113 **2.1 Biofilm inoculation**

114 The biofilm inoculation experiment was designed according to our previous study (Miao
115 et al., 2020). The cultivation device for the sample was located at the Qin Huai River in Nanjing,

116 Eastern China. All incubation devices were secured to a depth of 50 cm to receive the same light
 117 output and intensity. Each device was cultured for 44 days (from 30 October 2020 to 7
 118 December 2020) to obtain mature biofilm (Wu et al., 2014, Battin et al., 2016). Water quality in
 119 the Qin Huai River was measured over the culture period (Table S1). The experimental devices
 120 with all cobblestones and river water in the cultivation station were taken to the lab for further
 121 experiment.

122 2. 2 Laboratory experiment design

123 Flowing artificial water tanks (160 cm long, 20 cm wide, and 30 cm high) were designed
 124 for indoor adaptation of mature biofilms in a greenhouse at 18 ± 2 °C with natural light. The tanks
 125 were equipped with a pump to modify the water conditions (Figure S1). The flow rate in our
 126 culturing device was kept at 0.014 m/s controlled by a pump (BT100-1L, China) to create
 127 favorable conditions for biofilm adaptation (Liao et al., 2018).

128 In the laboratory experiment, 5ml/L nutrient solution/water (Table S2) was added weekly
 129 to the water tank for the adaptation of biofilms (Hou et al., 2019). After 2 weeks of adaptations,
 130 all cobblestones with biofilm were distributed in three parts. One-third of the cobblestones were
 131 kept in the tank with water as a control group, and one-third of the cobblestones were transferred
 132 to another tank for 25 days of desiccation and subsequent rewetting; as well the rest of the third
 133 was transferred to another tank for 90 days of desiccation and subsequent rewetting.

134 The selected duration of the non-flow periods fall within the range for the non-flow
 135 period reported for other IRES and artificial streams (20~100 days) (Fazi et al., 2013) (Acuña et
 136 al., 2015). Herein, 25 days of desiccation with 20 days of rewetting (expressed as 25-Rewetting)
 137 and desiccation for 90 days with 20 days of rewetting (expressed as 90-Rewetting) were
 138 conducted in the alternation of desiccation and rewetting experiments (Figure 1). Before
 139 desiccation, surface and free pore water were drained from the experimental tanks following the
 140 procedures in previous study (Zlatanović et al., 2018). After drying, the re-equipment of the
 141 biofilm was carried out by ascending reconstruction of small flows, avoiding destroy the biofilm
 142 on the surface of the cobblestones. Then, the water column was filled to the control level using
 143 the pump (Zlatanović et al., 2018). Samples were taken between the control group and the
 144 experimental group on days 0, 1, 3, 5, 7, 10, 25, and 90 of the non-flow periods, and in the
 145 experimental group on days 1, 3, 5, 7, 10, and 20 of the rewetting periods to measure various
 146 indicator variables (Table S3). At each sampling time, the pump was stopped, and a sterile brush
 147 and tweezers were used to collect the biofilms from the cobblestone surfaces (Liao et al., 2018,
 148 Liao et al., 2019).

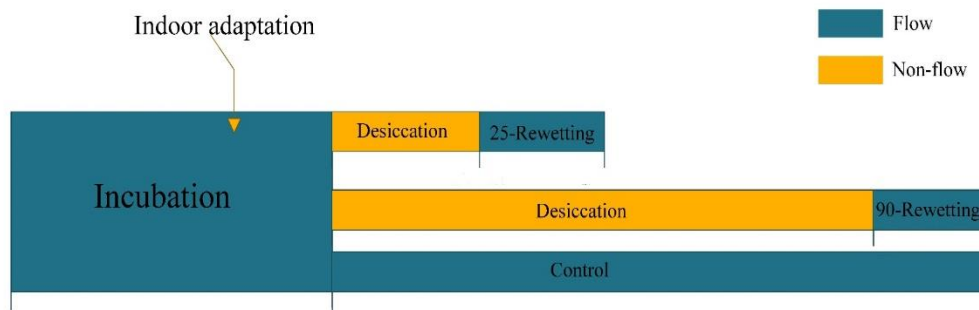


Figure 1. The alternation of desiccation and rewetting experiment time axis.

149 2.3 The biomass and morphology of biofilm

150 The biomass of biofilms, represented by ash-free dry weight (AFDW) was measured per
151 given area (30cm², 10-15 cobblestones). Biofilm samples were dried at 105 °C for 24 hrs and
152 then calcined at 450 °C for 4 hrs to estimate AFDW (Timoner et al., 2012).

153 Biofilm sample morphology was observed using an ESEM (QUANTA200, FEI
154 Company, The Netherlands) at various hydrologic stages(Yurudu, 2012). The biofilms on
155 cobblestones were attached to the sampling table with conductive adhesive, then placed in the
156 electron microscope sampling room and vacuumed and photographed in selected positions.

157 2.4 Characterization of the indicators of integrated function

158 This study identified indicators for the integrated function of biofilms, including GPP,
159 CR, and AI.

160 The AI is defined as the ratio AFDW/chl-a, which can reflect the shifts in dominance of
161 functional groups (i.e., AI>200 indicates a high proportion of heterotrophic) (Delgado et al.,
162 2017). The chlorophyll content of biofilm was determined with a portable pulse amplitude-
163 modulated fluorometer (PGYTO-PAM; WALZ, Effeltrich, Germany) (Hou et al., 2019,
164 Schreiber et al., 2002).

165 Ecosystem metabolism governs the fixation and mineralization of organic carbon (C) in
166 streams and is quantitatively expressed by the GPP: CR ratio (Schreiber et al., 2002). We
167 followed the approach from previous studies (Acuña et al., 2008) to estimate the biofilm
168 metabolism from the drop and rise in dissolved oxygen concentration, which was widely used in
169 ecosystem metabolism studies in rivers and streams (Gómez-Gener et al., 2016, Bott et al.,
170 1997). We used square recirculating chambers (24cm long, 19cm wide, 18cm high) to estimate
171 biofilm oxygen production and consumption(Bott et al., 1997). The chambers were equipped
172 with a submersible pump that recirculated water, avoiding the generation of low diffusion areas
173 within the chamber. The CR and GPP were measured for 120 minutes in constant dark and
174 brightness conditions, respectively. Dissolved oxygen was recorded at 10-min intervals with
175 oxygen sensors (miniDO2T Logger, PME, USA) (Liu et al., 2020, Adyel et al., 2017). Metabolic
176 rates were calculated as described by ACUÑA and others(Acuña et al., 2008, Zlatanović et al.,
177 2018). The GPP and CR were calculated as Eq. (1-2).

$$178 \quad CR = \left(\frac{dC_{treatment}}{dt} \right)_{night} * \left(\frac{V_{water}}{A_{sed}} \right) \quad (1)$$

$$179 \quad GPP = \left(\frac{dC_{treatment}}{dt} \right)_{day} * \left(\frac{V_{water}}{A_{sed}} \right) \quad (2)$$

180 where C_{treatment} is oxygen (mg/L), t is time(h), night and day represent the dissolved O₂
181 concentration data set used in the dark treatment and light treatment conditions (the measurement
182 time is 120 min), V_{water} is the total water volume (L) in the metabolism chamber, and A_{sed} is the
183 measuring bed surface(m²) (Zlatanović et al., 2018).

184 Based on the measurement of CR and GPP, the resistance and resilience of biofilms
185 during the experimental period were also calculated (Acuña et al., 2015). Resistance served as an
186 indicator of the capacity of stabilization and was calculated as the % decline in the variable
187 experienced between the last measurement before a disturbance and the first measurement after
188 the condition was restored. The resilience of biofilm was determined as the slope of the linear

189 functions of the relationship between each of the response variables and the time when flow
190 resume.

191 2.5 Carbon metabolism of biofilms

192 Biofilm samples from different hydrological stages were collected to determine their
193 carbon metabolic activities using Biolog Eco Plates (Biolog Inc., Hayward, CA, USA) (Zak et
194 al., 1994). The experimental methods are detailed in our previous study and given in the
195 Supplementary Information (Miao et al., 2021).

196 Based on the measured AWCD of Biolog Eco plate when biofilm metabolism is stable
197 (120h), the carbon metabolic functional diversity of biofilms were determined and represented
198 by three indices, Shannon-Wiener diversity index (H'), Simpson diversity index (D), and Pielou
199 evenness index (E) (Ge et al., 2018, Miao et al., 2019), and the formulas are presented in
200 Supplementary Information. At the same time, NMDS analysis was carried out based on
201 different measured values of 31 carbon sources when they reached metabolic stability (120h) in
202 each experimental cycle (Control, Desiccation, 25-Rewetting, and 90-Rewetting). The analytical
203 methodology can be found in the Statistical Analysis section.
204

205 2.6 Statistical analysis

206 All biochemical analyses of the biofilm samples during the desiccation and rewetting
207 were performed in triplicate, and the values are presented as the mean \pm standard deviation. A
208 further one-way ANOVA with ecological variables (AWCD or GPP and so on) was used to test
209 for significant differences. T-TEST analyzed the results of the control group and the desiccation
210 group. Graphs were plotted using Origin (Version 2018, Northampton, MA, USA).

211 Based on Bray-Curtis dissimilarities, NMDS analysis were used to study differences in
212 microbial functional composition in different treatments (Fasching et al., 2020). Then, an
213 ANOVA (permutational multivariate analysis of variance (PERMANOVA) was completed using
214 the Adonis function in the R Vegan package; (Oksanen et al., 2012). An analysis of carbon
215 metabolic diversity data was performed using the statistical environment R (R Core Team 2017)
216 and the packages ggplot2, ggsignif, and ggpubr (Wickham, 2009, Ahlmann-Eltze, 2019,
217 Kassambara, 2020).

218 3 Results

219 3.1 The water content and micromorphology of biofilms

220 During the alternation of desiccation and rewetting experiments, the water content of
221 biofilm was shown in Figure S2. After the desiccation started, the water content of biofilm
222 decreased quickly and was completely dehydrated 10 days later. When rewetting begins, the
223 water content of biofilm was rapidly resumed within the first two days, and reached the control
224 level after 10 days of recovery (t-test, $P > 0.05$), regardless of the duration of non-flow periods (25
225 days and 90 days).

226 The changes in morphology and structure of biofilm were introduced (Figure 2). The
227 micromorphological heterogeneity of biofilm is shown in the images of different map points.
228 With the increase of desiccant content, the phenomenon of disintegration of 3D structure and the

229 structural fragmentation of biofilm increases gradually (Figure 2a-e), leading to reduced the
 230 material transport channels of biofilm. As the rewetting begins, the fragmentation was gradually
 231 restored and the 3D structure of biofilms appears to be recovered (Figure 2f-k).

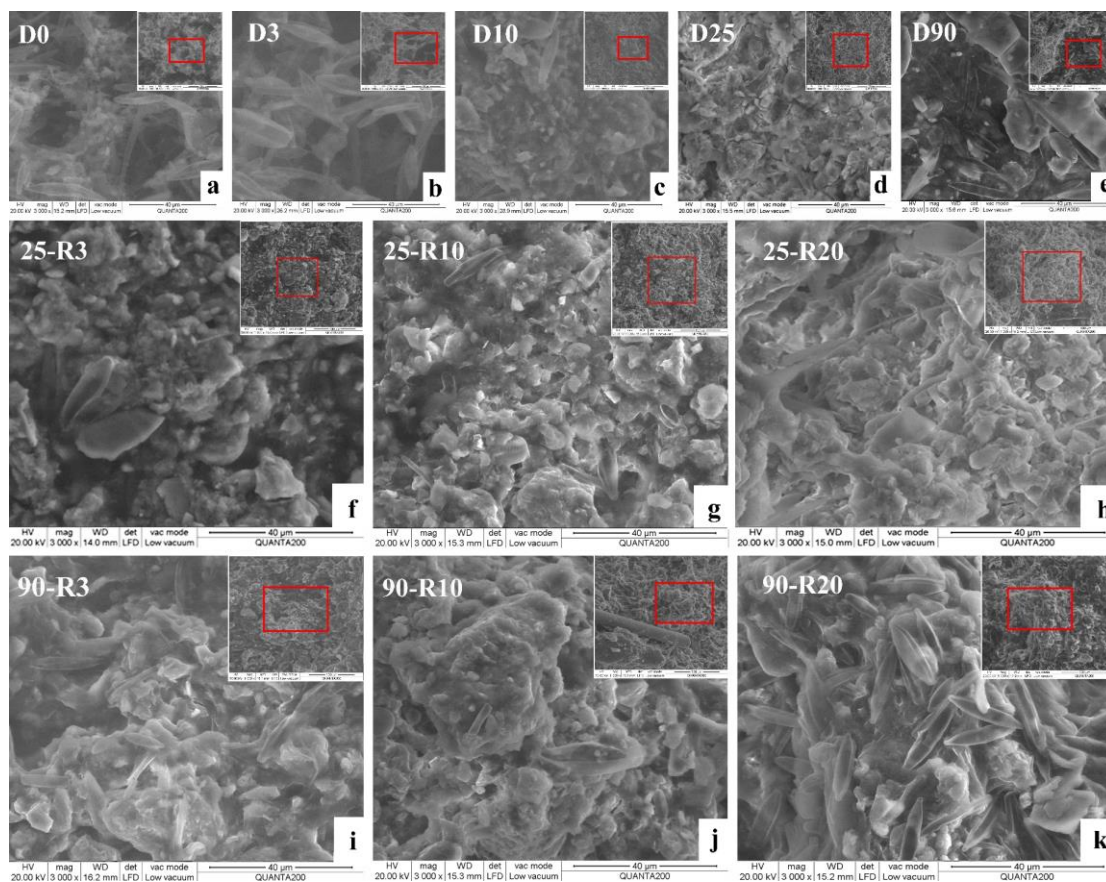


Figure 2. ESEM of biofilm during alternation of desiccation and rewetting. Each image is a detailed image in the red box at the top right. D0 is day 0 of desiccation and R0 is day 0 of rewetting.

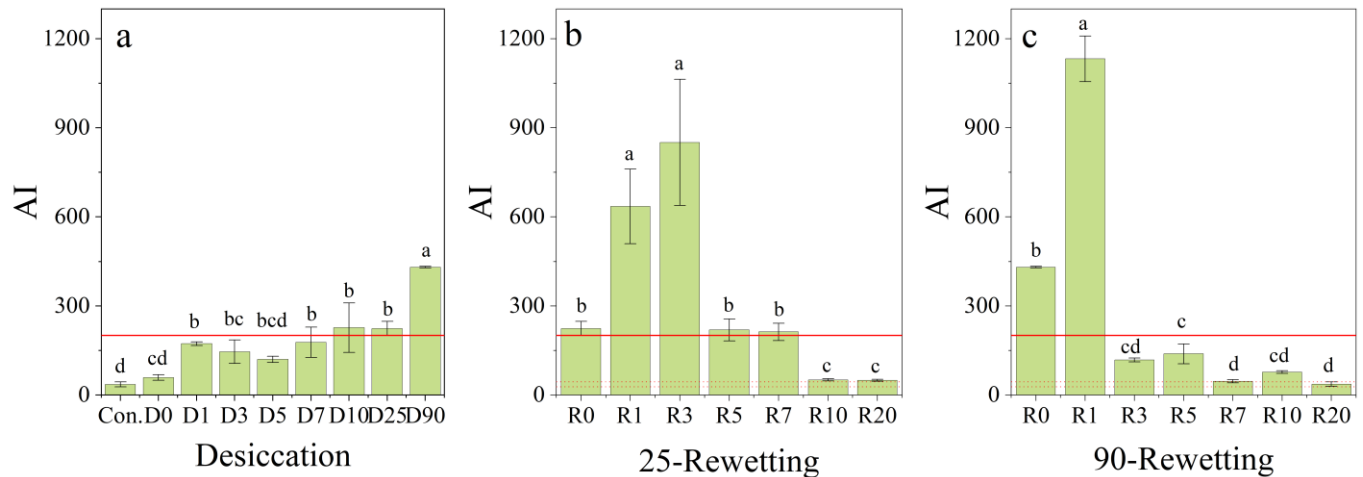
232 3.2 Biomass of biofilm

233 The AFDW of biofilm decreased rapidly with desiccation time and remained at the range
 234 of 0.986 and 1.433 mgcm⁻² after 7 days of desiccation, significantly different from that of control
 235 (t-test, p=0.000169; Figure S3a). The AFDW of biofilm recovered rapidly during rewetting and
 236 stabilized after 5 days (Figure S3b,c). While, the AFDW of biofilm can be restored to the control
 237 level for the 25-Rewetting group (Figure S3b), not for the 90-Rewetting group (Figure S3c).

238 With desiccation, chl-a concentration also decreased, and after 7 days, when the biofilm
 239 was completely dehydrated, it tended to be close to 0 mg/cm² (Figure S3d). Then, as the
 240 rewetting progressed, chl-a concentration was restored to 0.06 mg/cm² (close to the initial level,
 241 t-test, p>0.05) after 10 days (Figure S3e,f). In addition, chl-a content of the biofilm could reach a
 242 control level on the seventh day after longer desiccation but did not reach stability during the 20-
 243 day rewetting period.

244 3.3 Changes of the integrated function of biofilms

245 During desiccation, the value of AI increased with the duration of time, exceeding 200
 246 after 7 days (Figure 3a). This indicated a high proportion of heterotrophic in the biofilm system.
 247 When the rewetting started, the AI value raised significantly and then decreased rapidly as
 248 rewetting progresses, remaining below 200 after 3 days of rewetting (Figure. 3b,c). In addition,
 249 no matter the duration of desiccation, the AI was both recovered to the control level after 20 days
 250 of rewetting (t-test, $p > 0.05$, Figure 3b,c), indicating recovery of flow promoted autotrophy of
 251 biofilms.
 252

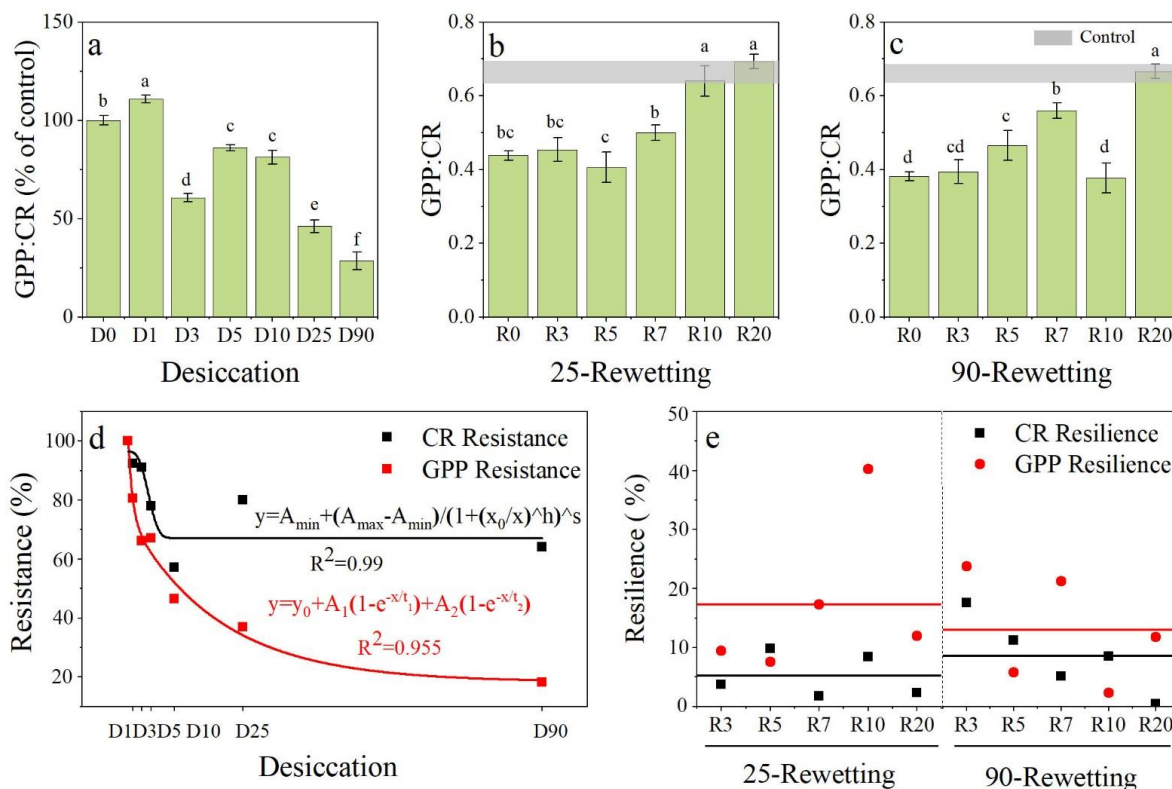


253 **Figure 3.** The value of AI (a-c) of biofilm during alternation of desiccation and rewetting. The lines at AI value 200
 254 (a, b, and c) indicate a high proportion of heterotrophic in the biofilm. The dotted lower and upper lines indicate the
 255 range of values for the control group(b, c). The error bars indicate standard deviation between parallel samples. The
 256 alphabetical letters abc indicate significant differences between samples.
 257

258 As shown in Figure S4, CR and GPP decreased gradually as the desiccation time
 259 increased (Figure S4 a,d), which was consistent with previous studies (Acuña et al., 2015,
 260 Zlatanović et al., 2018, Colls et al., 2019). The resistance of biofilms to desiccation was also
 261 calculated, as shown in Figure 4d. The resistance of CR has decreased significantly within the
 262 first 10 days of desiccation and then stabilized at $67.22 \pm 8.7\%$. The resistance of GPP was
 263 observed to continue declining, reaching nearly 0 after 90 days of desiccation. After longer
 264 desiccation, resistance to GPP continued to decrease, resulting in a significant decrease in
 265 GPP:CR (Figure 4a). The ecosystem metabolism of biofilm changed to heterotrophic
 266 metabolism. At the same time, there were differences in the best fitting models of the
 267 perturbation response of ecosystem metabolism (Figure 4d). The response of resistance to GPP
 268 was better described by an exponential curve with three parameters and X2 ($r^2 = 0.97326$), while
 269 CR was better described by a sigmoid logistic curve with four parameters ($r^2 = 0.99931$), a sign of
 270 its ecological threshold in the disturbance-response relationship (Acuña et al., 2015).

271 After further rewetting, CR gradually recovered to stable levels of control after 10 days
 272 (Figure S4b,c). Note that CR had a “brich effect” on the first day of the 90-Rewetting group
 273 (Figure S4) (Sabater et al., 2016, Muñoz et al., 2018). At higher resilience (Figure 4e), GPP
 274 increased with the prolongation of the rewetting cycle, however, at the end of the 20-day
 275 rewetting experiment, it had not yet reached stability (Figure S5e,f). There was no obvious
 276 pattern of the change of resilience in the rewetting experiment (Figure 4e). From the point of
 277 view of average resilience, the average resilience of GPP of biofilm decreased from 0.173 to

278 0.130 after longer desiccation (Figure 4e). Conversely, the average resilience of CR was from
 279 0.0522 and increased to 0.0856 (Figure 4e). The average resilience of GPP was always higher
 280 than that of CR.
 281



282 **Figure 4.** The ecosystem metabolism (represent by the ratio of GPP and CR, a-c) and the resistance of GPP and CR
 283 during desiccation (d), and the resilience of GPP and CR after rewetting (e). The shaded grey panels in b and c
 284 indicate control. The error bars indicate standard deviation between parallel samples. The alphabetical letters abc
 285 indicate significant differences between samples.
 286
 287
 288

289 3.4 The potential activity of carbon metabolism of biofilms

290 3.4.1 Effects of desiccation on the carbon metabolism of biofilms

291 During desiccation, the total AWCD value of biofilms decreased significantly at the
 292 beginning (t-test, $p < 0.05$) and then fluctuated steadily on the control level before the complete
 293 drought (t-test, $p > 0.05$) (Figure 5a). The potential activity of biofilm carbon metabolism
 294 decreased significantly lower than that of the control group (t-test, $p < 0.05$) after the biofilm was
 295 the complete drought (Figure 5a).

296 To evaluate the biofilm metabolic functions in a physiologically relevant approach, 31
 297 carbon sources were classified into six categories, including carbohydrates, amino acids,
 298 polymers, amines, carboxylic acids, and miscellaneous. Similar response patterns with the total
 299 AWCD were observed in the polymers, carbohydrates, amino acids, and carboxylic acids during
 300 desiccation (Figure S5a-d). Different response patterns were observed in the metabolism of

301 amines and miscellaneous (Figure 5b,c, and Figure S5e,f), with a significant increase in the two
302 carbon species during the first week of desiccation, followed by significant reductions (t-test,
303 $p < 0.01$, Figure 5b,c, and Figure S5e,f). The carbon consumption selectivity of biofilm
304 communities during the desiccation process is explained by the difference in the utilization ratio
305 of different carbon sources (Miao et al., 2021).

306 The results of the Shannon-Wiener diversity index (H'), Simpson diversity index (D), and
307 Pielou evenness index (E) of dynamic changes during desiccation are shown in Table S4. The
308 metabolic function diversity index showed a significant increase (t-test, P -value < 0.05) with the
309 desiccation period (Table S4). The high index indicated that desiccation promoted the metabolic
310 functional diversity of biofilm.

311 3.4.2 Effects of rewetting on the carbon metabolism of biofilms

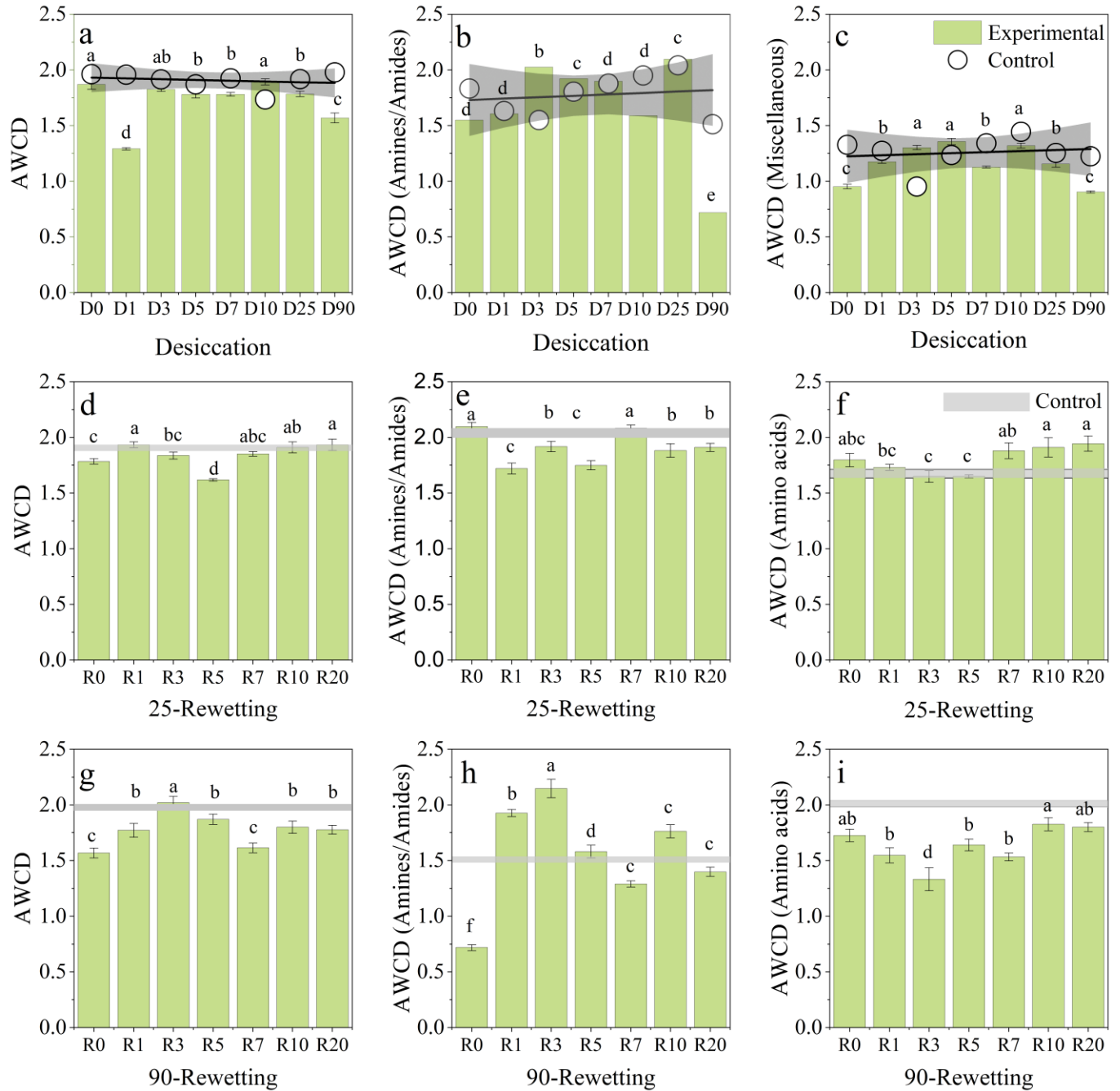
312 The dynamic changes of the total AWCD values during the rewetting experiment are
313 shown in Figure 5d,g. The same response patterns were observed in both processes, regardless of
314 the desiccation period (Figure 5d,g). During the first three days of the rewetting experiment, the
315 total AWCD value increased significantly and then fluctuated steadily (Figure 5d,g). The
316 difference here was that the biofilm stabilizes at the control level after 25 days of desiccation and
317 did not return to control after a longer desiccation period (Figure 5d, g). As for the different
318 carbon source specials of biofilms during the rewetting experiments, similar response patterns
319 with the total AWCD were observed for polymers, carbohydrates, miscellaneous, and carboxylic
320 acids (Figure S6a-d and Figure S7a-d). The metabolic response patterns of six different carbon
321 sources after long desiccation were more consistent with those of the total carbon source (Figure
322 S7a-d) as the total metabolic rate. The utilization of miscellaneous remained at the lowest levels,
323 indicating the selective carbon consumption of biofilm communities (Figure S6c and Figure S7c)
324 (Miao et al., 2021).

325 The metabolic functional diversity index did not show a significant difference at different
326 rewetting times (Table S5 and Table S6). It is noteworthy that the Shannon-Weiner diversity
327 index decreased significantly with the recovery of flow in group 25-Rewetting. Low index
328 suggested that rewetting reduced the metabolic function diversity of biofilms (ANOVA, P -value
329 < 0.01).

330

331

332



333
334
335
336
337
338
339
340

Figure 5. The total AWCD of biofilm (a, d, g) and specific carbon sources that differ from the overall pattern of metabolism (b, c, e, f, h, i) during the alternation of desiccation and rewetting. Linear fits of control data (a, b, c) indicate 95% confidential level. The shaded grey panels (d, e, f, g, h, i) indicate control. The error bars indicate standard deviation between parallel samples. The alphanumerical letters abc indicate significant differences between samples.

341

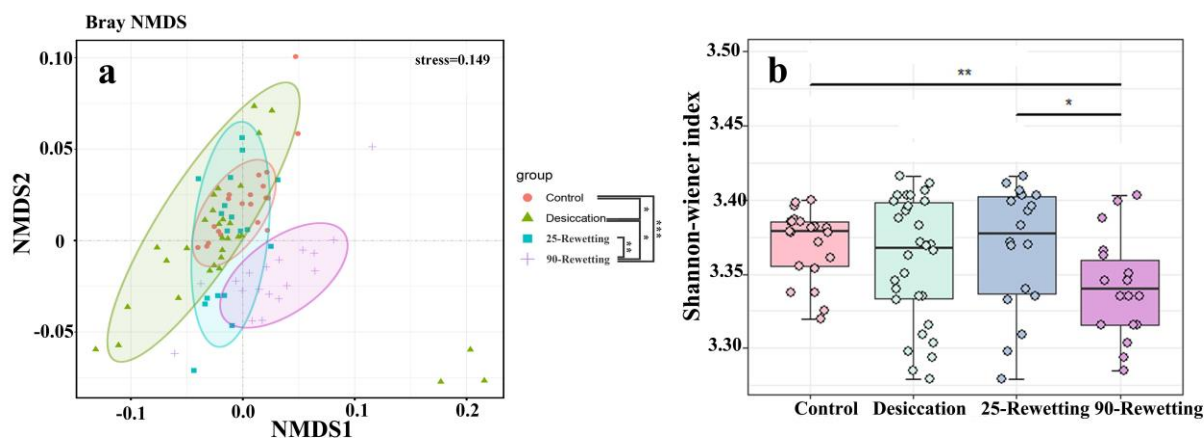
3.4.3 Effects of drought duration on carbon source utilization diversity

342

Microbial functions differed significantly between the 90-Rewetting group with other experimental stages (ANOVA using distance matrices, Bray-Curtis dissimilarity, $p < 0.05$, Figure

343

344 6a), while there was no significant difference between the 25-Rewetting group and the Control
 345 group (ANOVA using distance matrices, Bray-Curtis dissimilarity, $p > 0.05$, Figure 6a). The
 346 Shannon Diversity Index and the Simpson Diversity Index also showed that short-term
 347 desiccation had a reversible effect on biofilm metabolic diversity, while long-term desiccation
 348 could not (Figure 6b,c).
 349



350

351 **Figure 6.** Non-metric multidimensional scaling (NMDS) of all carbon sources ($n=31$) across experimental stages
 352 (Control, Desiccation, 25-Rewetting, 90-Rewetting) (a). Functional diversity of biofilms as the Shannon-wiener
 353 index (b) across the experimental stages (* $p < 0.05$, ** $p < 0.01$).

354 4 Discussion

355 In this study, the effects of different non-flow periods on the dynamic responses to flow
 356 recovery of biofilm metabolic activity were studied using biomass, integrated function indicators
 357 (AI and GPP:CR), and carbon metabolic activities. The first thing to be noted that the results of
 358 indoor simulation experiments should be carefully extrapolated to the field conditions. Although
 359 the irrelevant variables (light, temperature, and organic matters) during the desiccation can be
 360 eliminated through such controlled experiments, the disadvantage is that the environmental
 361 changes in natural waters are potentially more extreme and stressors can co-occur (Colls et al.,
 362 2019, Acuña et al., 2015).

363 4.1 Response patterns of the biomass and integrated function indicators of biofilm

364 The results showed that desiccation had a significant effect on the physical structure and
 365 biomass of biofilms, and biofilms were completely dehydrated after 10 days. Then, when the
 366 rewetting began, the water content, biomass, and micromorphology of biofilms responded
 367 rapidly (5-7 days). Regardless of how long the desiccation lasted, they can be returned to the
 368 control level (Timoner et al., 2012).

369 Different response patterns were observed for these two integrated function indicators. In
 370 the desiccation experiments, AI increased gradually to over 200, and GPPP:CR decreased
 371 gradually, indicating that the increase of the desiccation period would cause severe damage to
 372 the autotrophic group and promote heterotrophy of biofilms, consistent with previous studies
 373 (Acuña et al., 2015, Delgado et al., 2017). Decreases in AI values and increases in GPP:CR

374 values in rewetting experiments indicate that the major functional groups in the biofilms are
375 moving to the autotrophic group (Acuña et al., 2015). The dormancy mechanism of algae and an
376 increase in ambient temperature may partly explain why the recovery rate after 90 days of
377 desiccation is faster than after 25 days, contrary to our hypothesis that the response rate of
378 rewetting after 90 days desiccation is lower than that after 25 days.

379 Different disturbance-response relationships of GPP and CR during the desiccation and
380 rewetting were confirmed by different resistance and resilience of biofilm GPP and CR to flow
381 desiccation and flow recovery. The resistance of biofilm GPP was always lower than that of CR,
382 resulting in a continuous decrease in GPP:CR during desiccation, consistent with previous
383 studies (Timoner et al., 2012, Acuña et al., 2015). During the rewetting process, the average
384 resilience of the GPP was higher than that of CR, so that the ecosystem metabolism was
385 gradually restored and converted to an autotrophic body. In addition, the GPP disturbance-
386 response relationship was exponent while the relationship was sigmoid for CR, suggesting that
387 flow desiccation exhibit an immediate effect on autotrophs while the effect on heterotrophs was
388 delayed.

389 Timoner reports that the mechanism of rapid recovery of autotrophic groups from
390 rewetting may be related to the physiological restoration of dry algae and cyanobacteria that
391 remain on the surface of cobblestones (Timoner et al., 2012). So, the increase of effects of
392 duration and severity of the desiccation period may cause more damage to the recovery
393 mechanism, causing the decrease of the average resilience of GPP after long-term desiccation
394 (Figure 4e). The recovery mechanism of heterotrophic taxa may be the accumulation of organic
395 matter (dissolved or granular organic carbon) on the riverbed and in the biofilm during
396 desiccation, which may facilitate rapid respiration after rewetting (Colls et al., 2019). Therefore,
397 the accumulation of organic matter on the river bed increases with the prolongation of the
398 desiccation period, which may lead to an increase in the average resilience of CR after 90 days of
399 desiccation (Figure 4e). Besides, the enhanced CR on the first day of rewetting (Figure S4c)
400 resembles the “birch effect” (pulse of respiration on rewetting a dry soil), which may
401 significantly influence the carbon balance of the ecosystem (Sabater et al., 2016).

402 It should be noted that the biofilms’ CR achieved stability to the control after 10 days of
403 rewetting. However, at the end of the rewetting, the GPP continued to increase to the control
404 level but did not achieve stability, regardless of the duration of desiccation. It indicated that GPP
405 is strongly inhibited in desiccation, although the resilience of GPP is higher, it still needs a long
406 recovery time. This should be the focus of our subsequent experimental studies to determine the
407 recovery time and the final state of GPP.

408 4.2 Response patterns of biofilm carbon metabolism

409 Since the ecological indicators such as GPP, CR, and AI only reflect the integrated
410 functions of biofilms, the carbon metabolic activity determined by Biolog EcoPlate provides
411 more detailed information about the dynamic responses of biofilm metabolism to dry and wet
412 stress. During desiccation, the value of total AWCD decreased significantly on the first day and
413 then remained at the control level (Figure 5a). After the complete drought of biofilms, the total
414 AWCD began to decrease, while high potential carbon metabolism was observed after 25 and 90
415 days of desiccation. This phenomenon may be due to the existence of functional redundancy taxa
416 in biofilm communities. Several studies have found the high potential activity of enzymes during
417 desiccation (Pohlson et al., 2018, Su et al., 2020). This high potential activity increases during

418 desiccation, probably due to the continuous production of enzymes, or because the turnover rate
419 slows down (Acuña et al., 2015).

420 In this study, the length of the non-flow period resulted in different responses of carbon
421 metabolism in biofilms to flow recovery. After flow recovery, the biofilm from different non-
422 flow periods exhibited a similar response pattern, while the recovery rate of carbon metabolism
423 was slower after 90 days of desiccation. And the total AWCD was still below the control level at
424 the end of the rewetting (Figure 5d,g). This suggests that prolonged desiccation has irreversible
425 effects on carbon metabolism in biofilms. According to the response trends of different carbon
426 sources during rewetting, with the increase of desiccation, the response trends of all carbon
427 sources metabolism are gradually unified, which means that long-term desiccation may reduce
428 the existence of functional redundancy taxa, and the microorganism can recover from the
429 damaged state.

430 Meanwhile, the metabolism of amine and amino acid carbon sources has always shown a
431 different trend from that of the total metabolism. In addition, enzymes might already be available
432 when favorable conditions occur and are useful for rapid metabolism recovery in the initial phase
433 of rewetting. Carbon metabolism thus manifests itself as ‘stress recovery’, i.e., higher than the
434 control state and tended to over-compensate for their desiccation losses at the beginning of
435 rewetting (Pohlen et al., 2018). Previous study found that contrary to the activities of other
436 enzymes, the phenylalanine (amino acids) activity increased with increasing dryness (Gionchetta
437 et al., 2020). Therefore, we speculated that this may be the reason behind our results, which
438 show that only amino acid metabolic does not show ‘stress recovery’ at the initial stage of
439 rewetting.

440 From the point of the diversity of carbon metabolism, it can also be found that the time of
441 desiccation has significantly different effects on the metabolic function of biofilms (Fasching et
442 al., 2020). Rewetting after short-term desiccation can restore the carbon metabolism function of
443 biofilms in terms of activity and diversity (Figure 6). However, long-term desiccation has
444 irreversible effects, and even the recovery of water flow after long-term desiccation is an
445 interference with the arid system, which will further damage instead of recovery for biofilm
446 metabolism (Datry et al., 2018 , Ge et al., 2018).

447 4.3 Environmental implication

448 According to the results of the present study, different response patterns were observed
449 with the alternation of desiccation and rewetting of biofilms metabolism (GPP, CR, AI, and
450 carbon metabolism). During desiccation, the ecosystem metabolism of biofilms (PR ratio) was
451 inhibited due to the different resistance mechanisms of CR and GPP. In addition, we found that
452 after 90 days of prolonged desiccation, ecosystem metabolism could not recover stabilizable to
453 the control level within 20 days of rewetting (Figure 4b,c). And the total carbon metabolism of
454 biofilm was not recovered to the control level after long-term (90 days) desiccation, suggesting
455 that long-term desiccation and short-term desiccation have different effects on the carbon
456 metabolism function of IRES ecosystem. In addition, some carbon source categories, amine and
457 amino acid, have different response modes to rewetting response (Figure 5), indicating the
458 selectivity of carbon metabolism in biofilms, which have important effects on the carbon
459 biogeochemistry cycle of IRES.

460 These results provide some new insights for international decision-making on the
 461 restoration of ecological flows in IRES. From the perspective of the integrated function index
 462 and carbon metabolism, the ecological restoration of IRES should consider all river function
 463 indicators and select at least some important functional indexes based on the local ecological
 464 functions of IRES. Due to the different recovery times and degree of various biofilm functional
 465 indicators, to ensure the recovery of the overall ecological function of IRES, the index requiring
 466 a longer recovery time should be taken into consideration first.

467 **5 Conclusions**

468 In this study, the effects of duration of the non-flow period on the dynamic responses of biofilm
 469 metabolism to flow recovery were investigated. Based on the results, the following main
 470 conclusion were suggested:

- 471 1. The biofilm was completely dehydrated 10 days after desiccation, and the potential carbon
 472 metabolism of the biofilm remained highly active until the complete dehydration.
- 473 2. Most of the functional index of biofilms from the short-term desiccation treatments (25 days)
 474 were recovered to that of the control level after 20 days of rewetting.
- 475 3. The ecosystem metabolism and carbon metabolism of biofilms can not be restored to the
 476 control level after 90 days of desiccation, indicating that prolonged desiccation causes
 477 irreparable damage to the metabolic function of the biofilm.
- 478 4. Some carbon source categories, amine and amino acid showed different response modes to
 479 rewetting, indicating the selectivity of carbon metabolism in biofilms, which had important
 480 effects on the carbon biogeochemistry cycle of IRES.
- 481 5. In order to ensure the recovery of IRES's overall ecological function, the index requiring a
 482 longer recovery time should be taken into consideration first.

483 **Data Availability Statement**

484 All the data in this study has been uploaded as supplements for review purposes.

485 **Acknowledgement**

486 We are grateful for the grants for Project supported by the National Natural Science Foundation
 487 of China (No.51979075, and No. 52039003), the Fundamental Research Funds for the Central
 488 Universities (No. B210202053) and Jiangsu Province “333” project.

489 **References**

- 490 Acuña, V., Casellas, M., Corcoll, N., Timoner, X., Sabater, S., Naturvetenskapliga,
 491 F., . . . Gothenburg, U. (2015). Increasing extent of periods of no flow in intermittent
 492 waterways promotes heterotrophy. *Freshwater Biology*, 60(9), 1810-1823. Retrieved
 493 from <http://pku.summon.serialssolutions.com>
- 494 Acuña, V., Datry, T., Marshall, J., Barceló D., Dahm, C. N., Ginebreda, A., . . .
 495 Palmer, M. A. (2014). Why Should We Care About Temporary Waterways? *Science*,
 496 343(6175).
- 497 Acuña, V., Wolf, A., Uehlinger, U., & Tockner, K. (2008). Temperature dependence
 498 of stream benthic respiration in an Alpine river network under global warming.
 499 *Freshwater Biology*, 53(10), 2076-2088. doi:10.1111/J.1365-2427.2008.02028.X

- 500 Adyel, T. M., Hipsey, M. R., & Oldham, C. E. (2017). Temporal dynamics of
501 stormwater nutrient attenuation of an urban constructed wetland experiencing summer
502 low flows and macrophyte senescence. *Ecological Engineering*, *102*, 641-661.
503 doi:10.1016/J.ECOLENG.2016.12.026
- 504 Ahlmann-Eltze, C. (2019). Significance Brackets for 'ggplot2' [R package ggsignif
505 version 0.6.0]. In.
- 506 Battin, T. J., Besemer, K., Bengtsson, M. M., Romani, A. M., & Packmann, A. I.
507 (2016). The ecology and biogeochemistry of stream biofilms. *Nature Reviews*
508 *Microbiology*, *14*(4), 251-263. Retrieved from
509 <http://www.nature.com/articles/nrmicro.2016.15>
- 510 Bogan, M. T., Chester, E. T., Datry, T., Murphy, A. L., Robson, B. J., Ruhi, A., . . .
511 Whitney, J. E. (2017). Resistance, resilience and community recovery in intermittent
512 rivers and ephemeral streams. In (pp. 349-376).
- 513 Bott, T. L., Brock, J. T., Baatrup-Pedersen, A., Chambers, P. A., Dodds, W. K.,
514 Himbeault, K. T., . . . Wolfaardt, G. M. (1997). An evaluation of techniques for
515 measuring periphyton metabolism in chambers. *canadian journal of fisheries and aquatic*
516 *sciences*, *54*(3), 715-725. doi:10.1139/F96-323
- 517 Colls, M., Timoner, X., Font, C., Sabater, S., & Acuña, V. (2019). Effects of
518 Duration, Frequency, and Severity of the Non-flow Period on Stream Biofilm
519 Metabolism. *Ecosystems*, *22*(6), 1393-1405. Retrieved from
520 <http://link.springer.com/10.1007/s10021-019-00345-1>
- 521 Datry, T., Foulquier, A., Corti, R., von Schiller, D., Tockner, K., Mendoza-Lera,
522 C., . . . Zoppini, A. (2018). A global analysis of terrestrial plant litter dynamics in non-
523 perennial waterways. *Nature Geoscience*, *11*(7), 497-503. Retrieved from
524 <http://www.nature.com/articles/s41561-018-0134-4>
- 525 Delgado, C., Almeida, S. F. P., Elias, C. L., Ferreira, V., & Canhoto, C. (2017).
526 Response of biofilm growth to experimental warming in a temperate stream.
527 *Ecohydrology*, *10*(6), e1868. Retrieved from
528 <https://onlinelibrary.wiley.com/doi/10.1002/eco.1868>
- 529 Fabian, J., Zlatanović, S., Mutz, M., Grossart, H.-P., van Geldern, R., Ulrich, A., . . .
530 Premke, K. (2018). Environmental Control on Microbial Turnover of Leaf Carbon in
531 Streams – Ecological Function of Phototrophic-Heterotrophic Interactions. *Frontiers in*
532 *Microbiology*, *9*. Retrieved from
533 <https://www.frontiersin.org/article/10.3389/fmicb.2018.01044/full>
- 534 Fan, K., Delgado-Baquerizo, M., Guo, X., Wang, D., Zhu, Y.-g., & Chu, H. (2021).
535 Biodiversity of key-stone phylotypes determines crop production in a 4-decade
536 fertilization experiment. *The ISME Journal*, *15*(2), 550-561. Retrieved from
537 <http://www.nature.com/articles/s41396-020-00796-8>
- 538 Fasching, C., Akotoye, C., Bižić, M., Fonvielle, J., Ionescu, D., Mathavarajah,
539 S., . . . Xenopoulos, M. A. (2020). Linking stream microbial community functional genes
540 to dissolved organic matter and inorganic nutrients. *Limnology and Oceanography*,
541 *65*(S1). Retrieved from <https://onlinelibrary.wiley.com/doi/10.1002/lno.11356>
- 542 Fazi, S., Vázquez, E., Casamayor, E. O., Amalfitano, S., Butturini, A., & Smidt, H.
543 (2013). Stream hydrological fragmentation drives bacterioplankton community
544 composition. *PloS one*, *8*(5), e64109-e64109. Retrieved from
545 <http://pku.summon.serialssolutions.com>

- 546 Feng, L., He, L., Jiang, S., Chen, J., Zhou, C., Qian, Z.-J., . . . Li, C. (2020).
547 Investigating the composition and distribution of microplastics surface biofilms in coral
548 areas. *Chemosphere*, 252, 126565. Retrieved from
549 <https://linkinghub.elsevier.com/retrieve/pii/S004565352030758X>
- 550 Ge, Z., Du, H., Gao, Y., & Qiu, W. (2018). Analysis on Metabolic Functions of
551 Stored Rice Microbial Communities by BIOLOG ECO Microplates. *Frontiers in*
552 *Microbiology*, 9. Retrieved from
553 <https://www.frontiersin.org/article/10.3389/fmicb.2018.01375/full>
- 554 Gionchetta, G., Artigas, J., Arias Real, R., Oliva, F., & Romaní, A. M. (2020).
555 Multi - model assessment of hydrological and environmental impacts on streambed
556 microbes in Mediterranean catchments. *Environmental Microbiology*, 22(6), 2213-2229.
557 Retrieved from <https://onlinelibrary.wiley.com/doi/10.1111/1462-2920.14990>
- 558 Gionchetta, G., Romaní A. M., Oliva, F., & Artigas, J. (2019). Distinct responses
559 from bacterial, archaeal and fungal streambed communities to severe hydrological
560 disturbances. *Scientific Reports*, 9(1). Retrieved from
561 <http://www.nature.com/articles/s41598-019-49832-4>
- 562 Gómez-Gener, L., Obrador, B., Marcé R., Acuña, V., Catalán, N., Casas-Ruiz, J.
563 P., . . . von Schiller, D. (2016). When Water Vanishes: Magnitude and Regulation of
564 Carbon Dioxide Emissions from Dry Temporary Streams. *Ecosystems*, 19(4), 710-723.
565 Retrieved from <http://link.springer.com/10.1007/s10021-016-9963-4>
- 566 Hou, J., Li, T., Miao, L., You, G., Xu, Y., & Liu, S. (2019). Effects of titanium
567 dioxide nanoparticles on algal and bacterial communities in periphytic biofilms.
568 *Environmental Pollution*, 251, 407-414. Retrieved from
569 <https://linkinghub.elsevier.com/retrieve/pii/S0269749119302982>
- 570 Kassambara, A. (2020). 'ggplot2' Based Publication Ready Plots [R package ggpubr
571 version 0.4.0]. In.
- 572 Liao, K., Bai, Y., Huo, Y., Jian, Z., Hu, W., Zhao, C., & Qu, J. (2018). Integrating
573 microbial biomass, composition and function to discern the level of anthropogenic
574 activity in a river ecosystem. *Environment International*, 116, 147-155. Retrieved from
575 <https://linkinghub.elsevier.com/retrieve/pii/S016041201732086X>
- 576 Liao, K., Bai, Y., Huo, Y., Jian, Z., Hu, W., Zhao, C., & Qu, J. (2019). Use of
577 convertible flow cells to simulate the impacts of anthropogenic activities on river biofilm
578 bacterial communities. *Science of The Total Environment*, 653, 148-156. Retrieved from
579 <https://linkinghub.elsevier.com/retrieve/pii/S0048969718342621>
- 580 Liu, S., Wang, C., Hou, J., Wang, P., & Miao, L. (2020). Effects of Ag NPs on
581 denitrification in suspended sediments via inhibiting microbial electron behaviors. *Water*
582 *Research*, 171, 115436. Retrieved from
583 <https://linkinghub.elsevier.com/retrieve/pii/S0043135419312138>
- 584 Lv, T., Carvalho, P. N., Zhang, L., Zhang, Y., Button, M., Arias, C. A., . . . Brix, H.
585 (2017). Functionality of microbial communities in constructed wetlands used for
586 pesticide remediation: Influence of system design and sampling strategy. *Water*
587 *Research*, 110, 241-251. Retrieved from
588 <https://linkinghub.elsevier.com/retrieve/pii/S0043135416309617>
- 589 Messenger, M. L., Lehner, B., Cockburn, C., Lamouroux, N., Pella, H., Snelder,
590 T., . . . Datry, T. (2021). Global prevalence of non-perennial rivers and streams. *Nature*,
591 594(7863), 391-397. Retrieved from <http://www.nature.com/articles/s41586-021-03565-5>

- 592 Miao, L., Guo, S., Liu, Z., Liu, S., You, G., Qu, H., & Hou, J. (2019). Effects of
593 Nanoplastics on Freshwater Biofilm Microbial Metabolic Functions as Determined by
594 BIOLOG ECO Microplates. *International journal of environmental research and public
595 health*, 16(23), 4639. Retrieved from <http://pku.summon.serialssolutions.com>
- 596 Miao, L., Wang, C., Adyel, T. M., Wu, J., Liu, Z., You, G., . . . Hou, J. (2020).
597 Microbial carbon metabolic functions of biofilms on plastic debris influenced by the
598 substrate types and environmental factors. *Environment International*, 143, 106007.
599 Retrieved from <https://linkinghub.elsevier.com/retrieve/pii/S0160412020319620>
- 600 Miao, L., Yu, Y., Adyel, T. M., Wang, C., Liu, Z., Liu, S., . . . Hou, J. (2021).
601 Distinct microbial metabolic activities of biofilms colonizing microplastics in three
602 freshwater ecosystems. *Journal of Hazardous Materials*, 403, 123577-123577. Retrieved
603 from <http://pku.summon.serialssolutions.com>
- 604 Muñoz, I., Abril, M., Casas-Ruiz, J. P., Casellas, M., Gómez-Gener, L., Marcé
605 R., . . . Acuña, V. (2018). Does the severity of non-flow periods influence ecosystem
606 structure and function of temporary streams? A mesocosm study. *Freshwater Biology*,
607 63(7), 613-625. Retrieved from <https://onlinelibrary.wiley.com/doi/10.1111/fwb.13098>
- 608 Navarro-Ortega, A., Acuña, V., Bellin, A., Burek, P., Cassiani, G., Choukr-Allah,
609 R., . . . Barceló D. (2015). Managing the effects of multiple stressors on aquatic
610 ecosystems under water scarcity. The GLOBAQUA project. *Science of The Total
611 Environment*, 503-504, 3-9. Retrieved from
612 <https://linkinghub.elsevier.com/retrieve/pii/S0048969714009541>
- 613 Oksanen, J., Blanchet, F. G., Kindt, R., Legendre, P., Minchin, P. R., O'Hara, R.
614 B., . . . Wagner, H. (2012). vegan: Community Ecology Package. In.
- 615 Pohlón, E., Rütz, N. K., Ekschmitt, K., & Marxsen, J. (2018). Recovery dynamics of
616 prokaryotes and extracellular enzymes during sediment rewetting after desiccation.
617 *Hydrobiologia*, 820(1), 255-266. Retrieved from
618 <http://link.springer.com/10.1007/s10750-018-3662-4>
- 619 Sabater, S., Timoner, X., Borrego, C., & Acuña, V. (2016). Stream Biofilm
620 Responses to Flow Intermittency: From Cells to Ecosystems. *Frontiers in Environmental
621 Science*, 4. Retrieved from
622 <http://journal.frontiersin.org/Article/10.3389/fenvs.2016.00014/abstract>
- 623 Schreiber, U., Müller, J. F., Haugg, A., & Gademann, R. (2002). New type of dual-
624 channel PAM chlorophyll fluorometer for highly sensitive water toxicity biotests.
625 *photosynthesis research*, 74(3), 317-330. doi:10.1023/A:1021276003145
- 626 Shumilova, O., Zak, D., Datry, T., Schiller, D., Corti, R., Foulquier, A., . . . Zarfl, C.
627 (2019). Simulating rewetting events in intermittent rivers and ephemeral streams: A
628 global analysis of leached nutrients and organic matter. *Global Change Biology*, 25(5),
629 1591-1611. Retrieved from <https://onlinelibrary.wiley.com/doi/10.1111/gcb.14537>
- 630 Steven, B., Phillips, M. L., Belnap, J., Gallegos-Graves, L. V., Kuske, C. R., &
631 Reed, S. C. (2021). Resistance, Resilience, and Recovery of Dryland Soil Bacterial
632 Communities Across Multiple Disturbances. *Frontiers in Microbiology*, 12. Retrieved
633 from <https://www.frontiersin.org/articles/10.3389/fmicb.2021.648455/full>
- 634 Su, X., Su, X., Zhou, G., Du, Z., Yang, S., Ni, M., . . . Deng, J. (2020). Drought
635 accelerated recalcitrant carbon loss by changing soil aggregation and microbial
636 communities in a subtropical forest. *soil biology & biochemistry*, 148, 107898. Retrieved
637 from <http://pku.summon.serialssolutions.com>

- 638 Sun, R., Xu, Y., Wu, Y., Tang, J., Esquivel-Elizondo, S., Kerr, P. G., . . . Liu, J.
639 (2021). Functional sustainability of nutrient accumulation by periphytic biofilm under
640 temperature fluctuations. *Environmental technology*, 42(8), 1145-1154. Retrieved from
641 <http://pku.summon.serialssolutions.com>
- 642 Timoner, X., Acuña, V., Von Schiller, D., & Sabater, S. (2012). Functional
643 responses of stream biofilms to flow cessation, desiccation and rewetting. *Freshwater*
644 *Biology*, 57(8), 1565-1578. Retrieved from
645 <https://onlinelibrary.wiley.com/doi/10.1111/j.1365-2427.2012.02818.x>
- 646 Wickham, H. (2009). *ggplot2: Elegant Graphics for Data Analysis*.
- 647 Wu, Y., Xia, L., Yu, Z., Shabbir, S., & Kerr, P. G. (2014). In situ bioremediation of
648 surface waters by periphytons. *Bioresource Technology*, 151, 367-372. Retrieved from
649 <https://linkinghub.elsevier.com/retrieve/pii/S0960852413016751>
- 650 Yurudu, N. O. S. (2012). Study of biofilm associated bacteria on polyvinyl chloride,
651 stainless steel and glass surfaces in a model cooling tower system with different
652 microbiological methods. *iufs journal of biology*, 71(1), 63-76.
- 653 Zak, J. C., Willig, M. R., Moorhead, D. L., & Wildman, H. G. (1994). Functional
654 diversity of microbial communities: A quantitative approach. *soil biology &*
655 *biochemistry*, 26(9), 1101-1108. doi:10.1016/0038-0717(94)90131-7
- 656 Zlatanović, S., Fabian, J., Premke, K., & Mutz, M. (2018). Shading and sediment
657 structure effects on stream metabolism resistance and resilience to infrequent droughts.
658 *Science of The Total Environment*, 621, 1233-1242. Retrieved from
659 <https://linkinghub.elsevier.com/retrieve/pii/S0048969717328085>
- 660
- 661

662 **Figure 1.** The alternation of desiccation and rewetting experiment time axis

663 **Figure 2.** ESEM of biofilm during alternation of desiccation and rewetting. Each image is a
664 detailed image in the red box at the top right. D0 is day 0 of desiccation and R0 is day 0 of
665 rewetting.

666 **Figure 3.** The value of AI (a-c) of biofilm during alternation of desiccation and rewetting. The
667 lines at AI value 200 (a, b, and c) indicate a high proportion of heterotrophic in the biofilm. The
668 dotted lower and upper lines indicate the range of values for the control group(b, c). The error
669 bars indicate standard deviation between parallel samples. The alphabetical letters abc indicate
670 significant differences between samples.

671 **Figure 4.** The ecosystem metabolism (represented by the ratio of GPP and CR, a-c) and the
672 resistance of GPP and CR during desiccation (d), and the resilience of GPP and CR after
673 rewetting (e). The shaded grey panels in b and c indicate control. The error bars indicate standard
674 deviation between parallel samples. The alphabetical letters abc indicate significant differences
675 between samples.

676 **Figure 5.** The total AWCD of biofilm (a, d, g) and specific carbon sources that differ from the
677 overall pattern of metabolism (b, c, e, f, h, i) during the alternation of desiccation and rewetting.
678 Linear fits of control data (a, b, c) indicate 95% confidence level. The shaded grey panels (d, e,
679 f, g, h, i) indicate control. The error bars indicate standard deviation between parallel samples.
680 The alphabetical letters abc indicate significant differences between samples.

681 **Figure 6.** Non-metric multidimensional scaling (NMDS) of all carbon sources (n=31) across
682 experimental stages (Control, Desiccation, 25-Rewetting, 90-Rewetting) (a). Functional diversity
683 of biofilms as the Shannon-wiener index (b) across the experimental stages (* $p < 0.05$, ** $p <$
684 0.01).
685